Structural Engineering and Mechanics, Vol. 17, No. 3-4 (2004) 409-428
DOI: http://dx.doi.org/10.12989/sem.2004.17.3_4.409

Holder exponent analysis for discontinuity detection

Hoon Sohn†, Amy N. Robertson† and Charles R. Farrar†

Weapon Response Group, Engineering Sciences and Applications Division,
Los Alamos National Laboratory, Los Alamos, New Mexico 87545, USA

(Received October 1, 2002, Accepted August 27, 2003)

Abstract. In this paper, a Holder exponent, a measure of the degree to which a signal is differentiable, is presented to detect the presence of a discontinuity and when the discontinuity occurs in a dynamic signal. This discontinuity detection has potential applications to structural health monitoring because discontinuities are often introduced into dynamic response data as a result of certain types of damage. Wavelet transforms are incorporated with the Holder exponent to capture the time varying nature of discontinuities, and a classification procedure is developed to quantify when changes in the Holder exponent are significant. The proposed Holder exponent analysis is applied to various experimental signals to reveal underlying damage causing events from the signals. Signals being analyzed include acceleration response of a mechanical system with a rattling internal part, acceleration signals of a three-story building model with a loosing bolt, and strain records of an in-situ bridge during construction. The experimental results presented in this paper demonstrate that the Holder exponent can be an effective tool for identifying certain types of events that introduce discontinuities into the measured dynamic response data.

Key words: holder exponent; structural health monitoring; discontinuity detection; wavelet transform.

1. Introduction

In recent years, there have been increased economic and life-safety demands to continuously monitor the conditions and long-term deterioration of structures and mechanical assemblies to ensure their safety and adequate performance throughout their life spans. Structural health monitoring has applications to almost all engineering structures and mechanical systems including defense hardware, civil infrastructure, buildings, manufacturing equipments, and commercial aerospace and automotive systems. These increasing economic and safety concerns have initiated numerous structural health monitoring research throughout various engineering disciplines.

A recent literature review by the authors has revealed that although significant advances have been made in sensing and data acquisition technologies, much research work in signal processing and data interrogation is certainly a requisite (Sohn *et al.* 2003). For instance, 16 million US dollars are spent to install 600 various types of instrumentations including accelerometers, strain gauges, anemometers, thermocouples, GPS systems and etc. into the Tsing Ma Suspension Bridge in Hong Kong, which was completed in May, 1997 (Wong *et al.* 2000). However, little investigation has been done regarding how to utilize the tremendous amount of data that these sensors are constantly

† Technical Staff Member

producing. A personal communication with the local authorities indicates that they are overwhelmed by a large set of these continuously collected data.

Recent advances in micro-electromechanical system (MEMS) sensors and fiber optic sensors clearly demonstrate that the deployment of a dense array of sensors at an affordable price would be feasible in the next 5 to 10 years. The question that remains to be solved is how to best utilize a large amount of measured response data and extract information useful for a specific application. Furthermore, the increasing size of recorded data not only makes it difficult to transmit all the signals to a central storage or monitoring facility but also demands significant time and effort analyzing the acquired data. Vibration-based damage detection techniques assume that changes of the structure's integrity affect characteristics of the measured vibration signals enabling one to detect damage. Many current approaches to this problem involve methods that leave much to the interpretation of analysts. These methods may enable a trained eye to discern and identify damage, but these methods are not easily automated or objective.

The goal of this study is to develop a discontinuity detection technique based on the Holder exponent analysis, which can minimize unnecessary user interaction and can be potentially automated for the development of an autonomous continuous monitoring system. This application of the Holder exponent is not new in the analysis of time series data. For instance, Struzik (2001) uses the Holder exponent to characterize the underlying structure of a system that produces a time series of interest. The specific application is to financial data, where outliers and fluctuations in the Holder exponent value reveal interesting phenomena such as market crashes. Using the Holder exponent for discontinuity detection has also been shown to be useful in interpreting images (Shekarforoush *et al*. 1998). The edges in an image can be thought of as discontinuities and their identification can be used for finding abnormalities, removing noise, or even compressing the size of the image, because most of the information in an image is found in its edges. Holder exponents have even been used in one application of health monitoring. Hambaba and Huff (2000) use a wavelet transform to determine the Holder exponent value of a gear response at different scale levels. By fitting an Auto-Regressive Moving-Average (ARMA) model to the wavelet-transformed data, analysis of the residual error is used to indicate the presence of fatigue cracks in the gear. Peng *et al*. (2002) examine shaft orbits using the wavelet modulus maxima. The wavelet modulus is the absolute value of the wavelet transform and its maxima are ridges of high-valued coefficients that progress through the time-frequency plane. The Holder exponent values are extracted only for these maxima lines and then their distribution is used as input features to a neural network, which classifies the shaft orbit (including fault classification). These two applications are very different from the one presented in this paper. This paper will use the wavelet transform to obtain a time-based local Holder exponent function. Fluctuations in this function as demonstrated in Struzik (2001) will be useful for understanding and identifying outliers in the data. Hambaba and Huff (2002), on the other hand, are looking at the global regularity of the data at various scales and Peng *et al*. (2002) use the Holder exponent at specific points in time as a feature, rather than its variation in time.

2. Holder exponent analysis

A Holder or Lipschitz exponent, which provides a measure of a signal's regularity, is presented to detect the presence of a discontinuity and when the discontinuity occurs in a dynamic signal. The regularity of a signal is defined as the number of continuous derivatives that the signal possesses.

First the time varying nature of the Holder exponent is obtained based on a wavelet transform. Because discontinuity points have no continuous derivatives, these points are identified by locating time points where the Holder exponent value suddenly drops. Next, an automated classifier is developed to quantify when changes in this Holder exponent are significant. It should be noted that the proposed approach is very different from the one presented by Hambaba and Huff (2000). This paper will use the wavelet transform to obtain a time-based local Holder exponent function, and fluctuations in this function will be useful for understanding and identifying outliers in the data. Hambaba and Huff (2000), on the other hand, look at the global regularity of the data at various scales.

2.1 Wavelet analysis of signals

Wavelets have been gaining in popularity as the multi-scale transform of choice since their first influx into mainstream mathematics and engineering in the early 90's. Wavelets are mathematical functions that decompose a signal into its constituent parts using a set of wavelet basis functions. This decomposition is very similar to Fourier transforms, which use dilations of sinusoids as the bases. The family of basis functions used for wavelet analysis is created by both *dilations* (scaling) and *translations* (in time) of a "mother wavelet", thereby providing both time and frequency information about the signal being analyzed. There are many different functions that can be called wavelets. In this study, the Morlet wavelet is used for the family of basis functions. This wavelet, $\psi(t)$, is defined as:

$$\psi(t) = e^{(-\sigma^2 t^2 - i2\pi f_0 t)} \tag{1}$$

which is very similar to a sinusoid with a Gaussian envelope. The term f_o is the center frequency of the sinusoid and σ determines the width of the frequency band. Also, t is the time variable and i the imaginary value of $\sqrt{-1}$. The wavelet transform, $Wf(u, s)$, is obtained by convolving the signal $f(t)$ with the translations (u) and dilations (s) of the mother wavelet:

$$Wf(u, s) = \int_{-\infty}^{\infty} f(t) \frac{1}{\sqrt{s}} \psi^* \left(\frac{t-u}{s} \right) dt \tag{2}$$

where

$$\psi^*_{u,s}(t) = \frac{1}{\sqrt{s}} \psi \left(\frac{t-u}{s} \right) \tag{3}$$

The transform itself can be categorized as either discrete or continuous. By computing the continuous wavelet transform at integer values of the translation parameter, u, and only at dyadic values of the scale parameter, s, the most common form of the discrete wavelet transform is found. The discrete transform provides an efficient method for computing the wavelet transform, resulting in the fewest number of coefficients needed to characterize the signal without loss in reconstruction. This property makes the discrete transform popular in signal/image compression and data transmission applications. For analysis purposes, however, compactness and speed are not nearly as important as accuracy. The compact form of the discrete transform might allow singularities to go undetected unless they align themselves with the precise points in the time-scale space where the discrete transform is computed. The continuous transform supplies redundant information, but with

a finer resolution. Thus, for discontinuity detection presented here, a continuous wavelet transform is used so that a more precise localization of the discontinuity points can be found.

A common problem with wavelets is end-effects. End-effects are the errors in the wavelet transform resulting from performing a convolution on a finite-length signal. Any transform or filtering process that performs a convolution on a finite signal will suffer from errors caused by these end-effects. Zero-padding and mirroring of the signal are used in this paper to deal with this problem. The calculation of the Holder exponent is greatly improved when the end-effects are dealt with.

2.2 Characterization of the pointwise holder regularity for discontinuity detection

The resulting coefficients from the wavelet transform of a time domain signal, such as the acceleration response of a structure, can be represented in a two-dimensional time-scale map. Examination of the modulus of the wavelet transform shows that many of these coefficients are very small in magnitude. Large magnitude components, termed modulus maxima, will be present at time points where the most change in the signal has occurred. Jumps or singularities in the signal can therefore be identified by the presence of modulus maxima at specific time points in the wavelet map. Singularities are distinguishable from noise by the presence of modulus maxima at all of the scale levels for a given time point. Noise will produce maxima at the finer scales, but will not persist to the coarser scales. Mallat and Hwang (1992) first introduced a method for detecting singularities in a signal by examining the evolution of the maxima of the modulus of the wavelet transform across the scales. The decay of this maxima line can then be used to determine the regularity of the signal at a given time point. A less time consuming alternative to the extraction of the maxima line is to simply look at the decay of the wavelet modulus across the scales at a given time point. Points of large change in the signal will have large coefficients at all the different scales, thus having little decay. Features such as noise, however, only produce large coefficients in the finer scales and therefore would show more decay across all of the scales. The measure of this decay is the Holder exponent of the signal at a given time point.

The Holder exponent, also known as the Lipschitz exponent (Mallat and Hwang 1992) is a tool that provides information about the regularity of a signal. In essence, the regularity identifies to what order a function is differentiable. For instance, if a signal $f(t)$ is differentiable at $t = 0$ it has a Holder exponent of 1. If the signal is discontinuous but bounded in the neighborhood of $t = 0$, such as a step function, then the Holder exponent is 0. The Dirac Delta function then has a Holder exponent of -1 because it is unbounded at $t = 0$. It turns out that there is a relationship between the Holder exponent of a function and its derivatives and primitives. Taking the derivative of a function decreases its regularity by 1 and integrating increases it by 1.

For the applications in this paper, singularities are defined as points in the signal that are discontinuous. As discussed above, bounded discontinuities have a Holder exponent of 0. Therefore, measuring the regularity of the signal in time can be used to detect these singularities. The Holder exponent can pertain to the global regularity of a function, or it can be found locally. A common method for finding its value is through the use of the Fourier transform (Mallet and Hwang 1992). The asymptotic decay of a signal's frequency spectrum relates directly to the uniform Holder regularity. The Fourier transform approach only provides a measure of the minimum global regularity of the function, and cannot be used to find the regularity at a particular point in time. Wavelets, on the other hand, are well localized in time and can therefore provide an estimate of the

Holder regularity over both time intervals and at specific time points. The wavelet method for estimating the Holder exponent is similar to that of the Fourier transform. The wavelet provides a time-frequency map called the *scalogram*. By examining the decay of this map at specific points in time across all scales (frequencies), the point-wise Holder regularity of the signal can be determined.

The Holder regularity is defined as follows. Assume that a signal $f(t)$ can be approximated locally at t_0 by a polynomial of the form (Struzik 2001):

$$\begin{aligned} f(t) &= c_0 + c_1(t-t_0) + \ldots + c_n(t-t_0)^n + C|t-t_0|^{\alpha} \\ &= P_n(t-t_0) + C|t-t_0|^{\alpha} \end{aligned} \tag{4}$$

where P_n is a polynomial of order n and C is a coefficient. The term associated with the exponent α can be thought of as the residual that remains after fitting a polynomial of order n to the signal, or as the part of the signal that does not fit into an $n + 1$ term approximation. The local regularity of a function at t_0 can then characterized by this "Holder" exponent:

$$|f(t) - P_n(t-t_0)| \le C|t-t_0|^{\alpha} \tag{5}$$

In order to detect discontinuities, a transform is needed that ignores the polynomial part of the signal. A wavelet transform that has n-vanishing moments is able to ignore polynomials up to order n:

$$\int_{-\infty}^{\infty} t^n \psi(t)dt = 0 \tag{6}$$

Transformation of Eq. (5) using a wavelet with at least n vanishing moments then provides a method for extracting the values of the Holder exponent in time:

$$|Wf(u, s)| \le Cs^{\alpha} \tag{7}$$

where $Wf(u, s)$ is the wavelet transform at time translation u and scale s. The wavelet transform of the polynomial is zero and so what remains is a relationship between the wavelet transform of $f(t)$ and the error between the polynomial and $f(t)$, which relates to the regularity of the function. When a complex wavelet such as the Morlet wavelet is used, the resulting coefficients are also complex. Therefore, the magnitude of the modulus of the wavelet transform, called the scalogram, must be used to find the Holder exponent. As detailed in the next section, the exponent α can be calculated at a specific time point by finding the slope of the log of the scalogram at that time versus the log of the scale vector s.

The concept of the Holder exponent was first introduced in this paper in terms of the decay of the Fourier transform. It is logical therefore to wonder if a short-time Fourier transform (STFT) could be used to extract a time-varying Holder exponent function as well. In fact, any time-frequency transform can be used for Holder exponent extraction, but certain characteristics of the wavelet transform make it particularly well adapted for this application. Specifically, the decay of the wavelet basis functions in the frequency domain, which is associated with the number of vanishing moments, and the variability of the bandwidth of the wavelet transform in time and frequency. The order of the wavelet limits the degree of regularity that can be measured in a function. Therefore,

wavelets can be tuned to the signals that are being analyzed. Also, the variability of the time and frequency bandwidths provides a finer time resolution at the higher frequencies, which can be helpful in detecting the location of sudden changes in a signal in time.

The measurement of the regularity can be used to detect discontinuities in a signal. The easiest way to identify a discontinuity is by looking for a distinct downward jump in the regularity versus time plot. A discontinuous point should have a Holder exponent of zero, but resolution limitations of the wavelet transform will result in slightly different values. So, identifying areas where your Holder exponent dips from positive values towards zero, or below, will identify when the discontinuities in the signal occur. A procedure for identifying the discontinuities will be presented in the following section.

2.3 Extraction of the holder exponent

The steps for calculating the Holder exponent in time are as follows. First, take the wavelet transform of the given signal and take the absolute value of the resulting coefficients to obtain the wavelet transform modulus:

$$|Wf(u, s)| = \left| \int_{-\infty}^{\infty} f(t) \frac{1}{\sqrt{s}} \psi^* \left(\frac{t-u}{s} \right) dt \right| \tag{8}$$

Then, arrange the coefficients in a two-dimensional time-scale matrix. One dimension of the time-scale matrix (u) represents a different time point in the signal, and the other dimension denotes a different frequency scale (s). Take the first column, which represents the frequency spectrum of the signal at the first time point, and plot the log of it versus the scales, s, at which the wavelet transform was calculated. This procedure can be shown mathematically by taking the log of each side of Eq. (7):

$$\log|Wf(u, s)| = \log(C) + \alpha \log(s) \quad \text{and} \quad m = \frac{\log|Wf(u, s)|}{\log(s)} = \alpha \tag{9}$$

Ignoring the offset due to the coefficient C, the slope m is then the decay of the wavelet modulus across its scales. Negating the slope will give the decay versus the frequencies of the transform rather than the scales, due to the inverse relationship between scale and frequency. The Holder exponent α is then simply the slope m. This is the Holder exponent for the first time point in the signal. To find the Holder exponent at all time points, repeat this process for each time point of the wavelet modulus matrix.

2.4 Development of a discontinuity classifier

An automated classifier is created to detect the presence of discontinuities in the signals by identifying drops in the Holder exponent in time. The previous investigation by the authors indicates that looking at the depth of a drop in the Holder exponent is an effective way of assessing a discontinuity (Robertson *et al.* 2003a).

A threshold is set such that any drops that exceed this threshold are labeled as discontinuities. The threshold value is set using a portion of the data known to contain no discontinuities, and this portion of data is termed “normal” data. The procedure starts by finding all the local maxima and

minima of the Holder exponents in time for the normal signal. Then, drops in the Holder exponent values are calculated as the difference between a given minimum and the maximum immediately preceding it. Next, the threshold is determined by finding the largest drop under "normal" conditions and amplifying this number by a factor of 1.5. The procedure for determining the depths of the drops in the Holder exponent function is then repeated on the remaining data of interest. If any of the drops are 50% deeper than the biggest drop in the normal data, the time point is identified as a discontinuity location. It should be noted that this amplification factor is application specific, and this threshold can be altered to be more or less restrictive, based on the needs of the application. In Robertson *et al*. (2003b), a threshold value is established based on a more statistically rigorous technique called extreme value statistics. For the all examples presented in this paper, the value of 1.5, however, serves our purpose well.

In some instances, the dips in the Holder value are jagged with small oscillations. This property makes the estimation of the dip's depth a difficult task because the algorithm relies on comparing the local maxima and minima, which will now also appear in the small fluctuations in the dip itself. Therefore, it was decided to add the option of smoothing the Holder exponent values before performing the discontinuity detection algorithm by applying a low-pass moving average (MA) filter:

$$\alpha(k) = \frac{1}{m}\sum_{i=k}^{k+m}\alpha(i) \tag{10}$$

where $\alpha(i)$ is the Holder exponent values at the ith time point and m is the number of points used in the averaging. This filtering process effectively removes the oscillations in the dips and allows for an appropriate detection of the discontinuities.

3. Data interrogation of various signals

The effectiveness of the Holder exponent for detection discontinuities in signals is demonstrated in this section using three different types of signals. The first one is acceleration record obtained from a mechanical system with an internal rattling part. The second one is acceleration responses measured from a three-story building model near a loosened bolted joint. Finally, the discontinuity detection algorithm is applied to strain reading obtained during construction of the Singapore-Malaysia Second Link Bridge.

3.1 Acceleration time signals from a rattling mechanical system

This first example investigates the acceleration response of a mechanical structure subjected to a harmonic base excitation. The defense nature of the test structure precludes a detailed description of its geometry or material properties. Instead a structure that is conceptually similar is schematically shown in Fig. 1. The exterior container of the system is horizontally excited at 18 Hz, and the non-symmetric bumpers attached to two interior side walls of the container cause the internal mass to exhibit a rattle during one portion of the harmonic excitation.

Fig. 2 shows the response of the structure at three different excitation levels measured by accelerometers mounted on the outer structure in the in-axis and off-axis directions. The placement and orientations of the in-axis and off-axis accelerometers are shown in Fig. 1. The rattle produced by these impacts is evident in the sensor measurements that are off-axis from the excitation. The

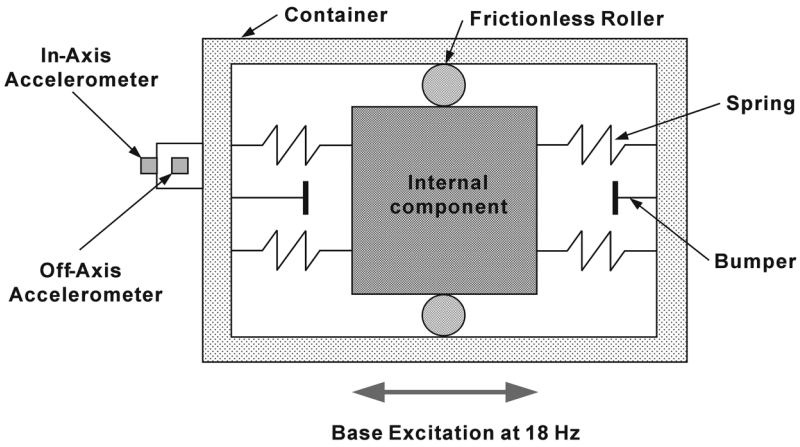

Fig. 1 A schematic diagram of a mechanical test structure that has a loose internal part and non-symmetric bumpers

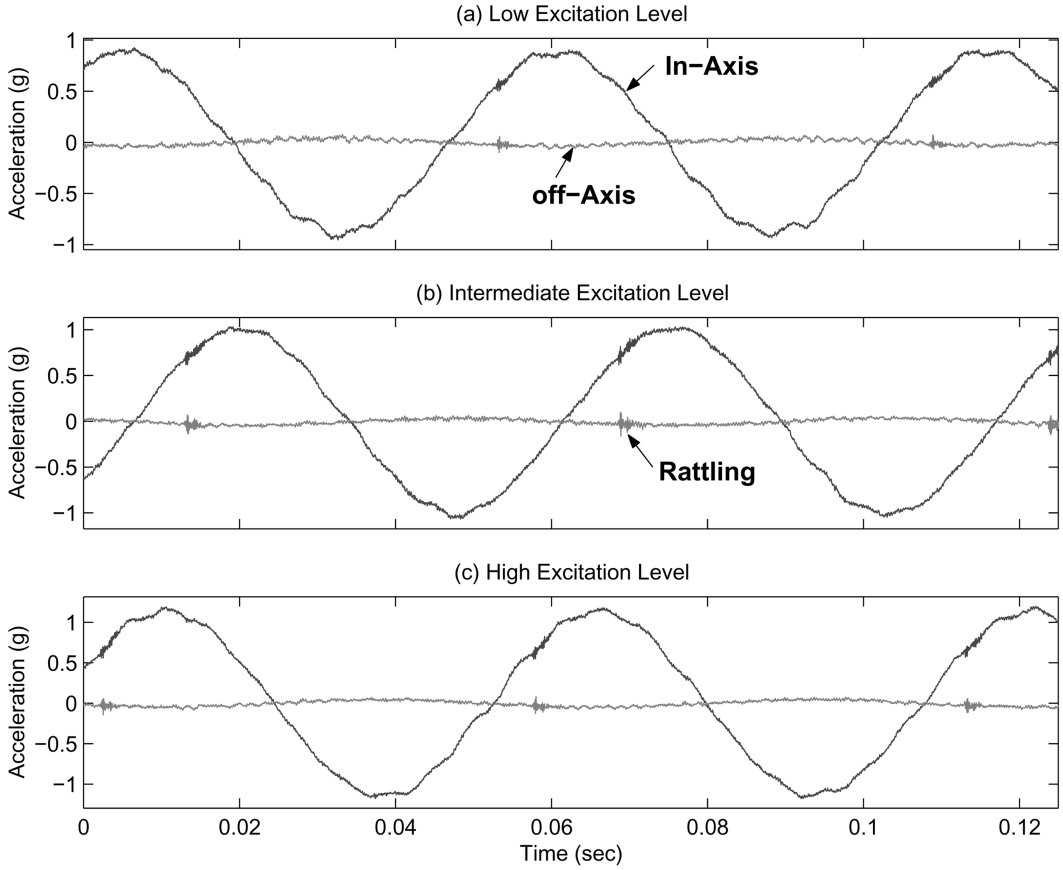

Fig. 2 Acceleration response of the test structure at three base excitation levels as measured in the in-axis and off-axis directions by accelerometers mounted on the outer structure

short oscillations of increased magnitude in these measurements are indicative of the rattle. For the lowest excitation level, the rattling is occurring near 5.33 and 10.89 milliseconds. Similar rattling can be observed for the intermediate and the highest excitation levels near 1.34, 6.88, and 12.39 milliseconds, and 0.25, 5.80, and 11.33 milliseconds, respectively. These same oscillations are not readily apparent in the in-axis data, particularly if one does not have the off-axis measurements for reference. The examination of the data from all three input levels shows that one can only see the rattle clearly in the off-axis measurements, and the lowest excitation level had the lowest signal to noise ratio, thus making observation of the rattle more difficult. The purpose of this application is to determine whether the presented technique can be used to identify the time when the rattle is occurring by looking only at the in-axis response measurements. For the acceleration signals analyzed in this example, 4096 acceleration time points are recorded for 0.125 seconds resulting in a sampling frequency of 3276 Hz.

First, a time-frequency information shown in Fig. 3 is obtained using a wavelet transform. The time locations of the rattling phenomena are clearly visible in this figure. A complex-valued Morlet wavelet with length 16 is used for the scalogram, and 256 scales are used between 0 Hz to the Nyquist frequency (1638 Hz). A larger width wavelet function increases the overall frequency

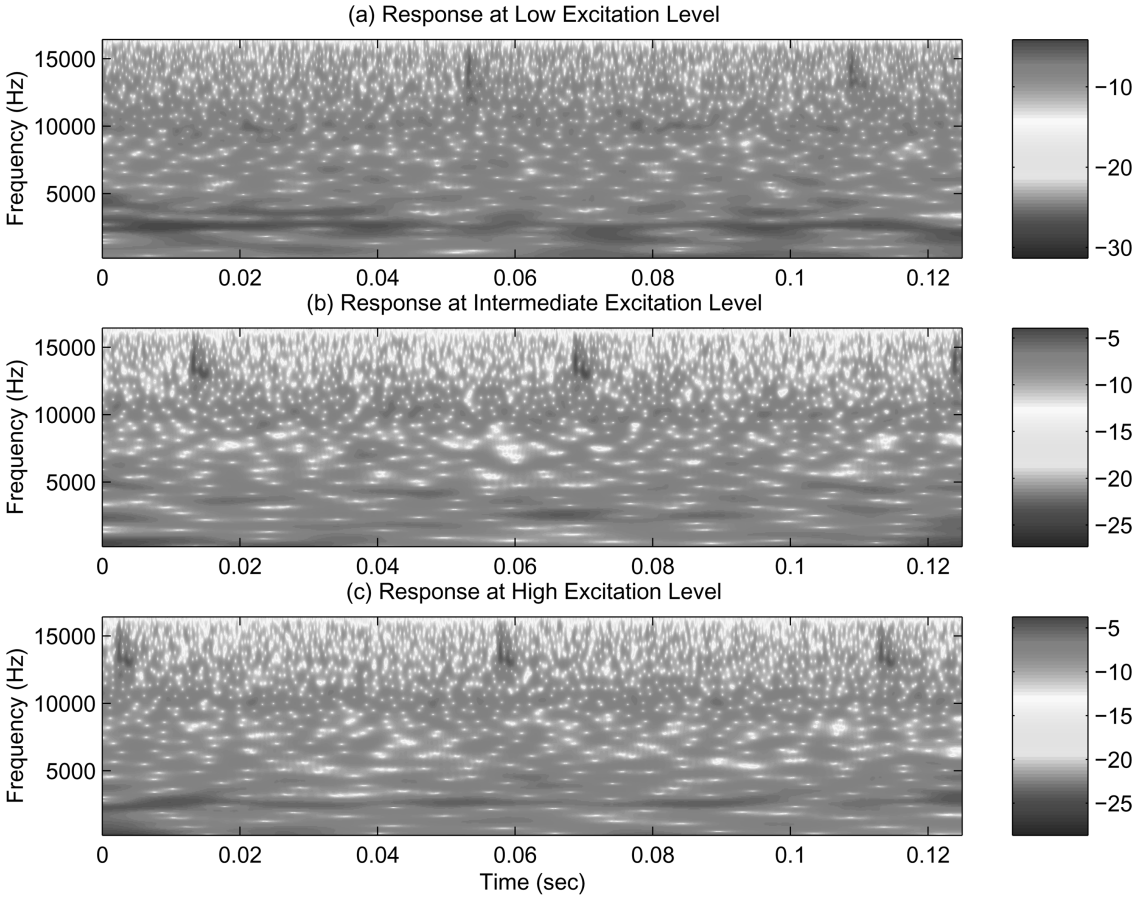

Fig. 3 The scalogram for the in-axis acceleration data subject to the three-excitation levels

resolution of the transform while decreasing the time resolution. The coarse time resolution acts as a smoothing filter decreasing the amount of spurious oscillation in the Holder exponent and bringing out changes associated with true discontinuities. To minimize the end effect of the wavelet transform, a continuous wavelet transform with mirroring is used in this example. The program for this mirrored wavelet computation is available at www.irccyn.ecnantes.fr/FracLab/Fraclab.html as part of Fractal Analysis Software, copyrighted by INRIA.

The next step is to transfer this visual interpretation of the images to a more automated identification procedure. For this purpose, the Holder exponent was extracted from the scalogram. Fig. 4 shows the Holder exponent obtained from the previous scalogram in Fig. 3. To smooth the plot of the Holder exponent, averaging with a moving window size of 8 was applied [see Eq. (10)]. The singularities associated with the rattle are clearly visible in this plot at each time they occur during the oscillatory cycles. Though the dips in the Holder exponent shown in Fig. 4 are fairly apparent to the naked eye, identification of them using an automated procedure is more difficult. The discontinuity classification algorithm described in the previous section was used to identify the locations of the rattle. The first 1000 time points of the lowest level response was used as the "normal data" to establish the threshold value for discontinuity detection. The threshold value was

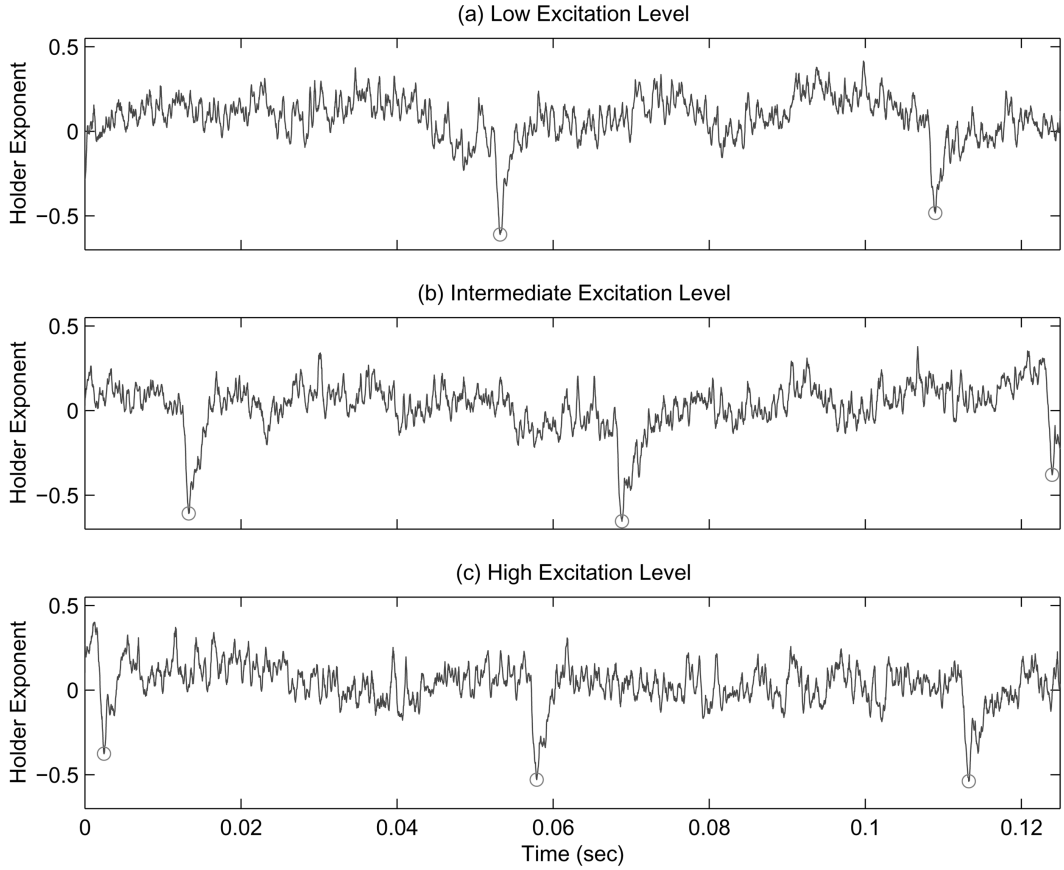

Fig. 4 The Holder exponent extracted from the scalogram of the in-axis acceleration data subjected to the three-excitation levels

then set at 150% of the largest dip in the normal data. Filtering using the moving average method effectively removed the spurious oscillations in the dips and allowed for a successful detection of the discontinuities as shown by the circles in Fig. 4. Although it is not reported here, a similar Holder exponent analysis is repeated using the spectrogram instead of the scalogram. However, the holder exponent extracted from the spectrogram failed to identify the rattle. It is speculated that because of the high-energy concentration in the low frequency range of the spectrogram, a frequency spreading into the higher frequency range associated the rattle did not change the values of the Holder exponent beyond natural fluctuation. Furthermore, the spectrogram was unable to provide a time resolution fine enough to accurately calculate the Holder exponent.

Third, an empirical mode decomposition (EMD) is applied to the signals. This fairly new signal processing technique decomposes a signal into a finite and often small number of intrinsic mode functions (IMFs) that admit well-behaved Hilbert transforms. Because the decomposition is based on the local characteristic time scale of the data, this method has been shown effective in processing nonlinear and nonstationary data (Huang *et al*. 1998). The Hilbert transforms of IMFs yield instantaneous frequencies as a function of time, thereby providing time-frequency information. Within an individual IMF, the instantaneous frequency can vary, but the instantaneous frequencies

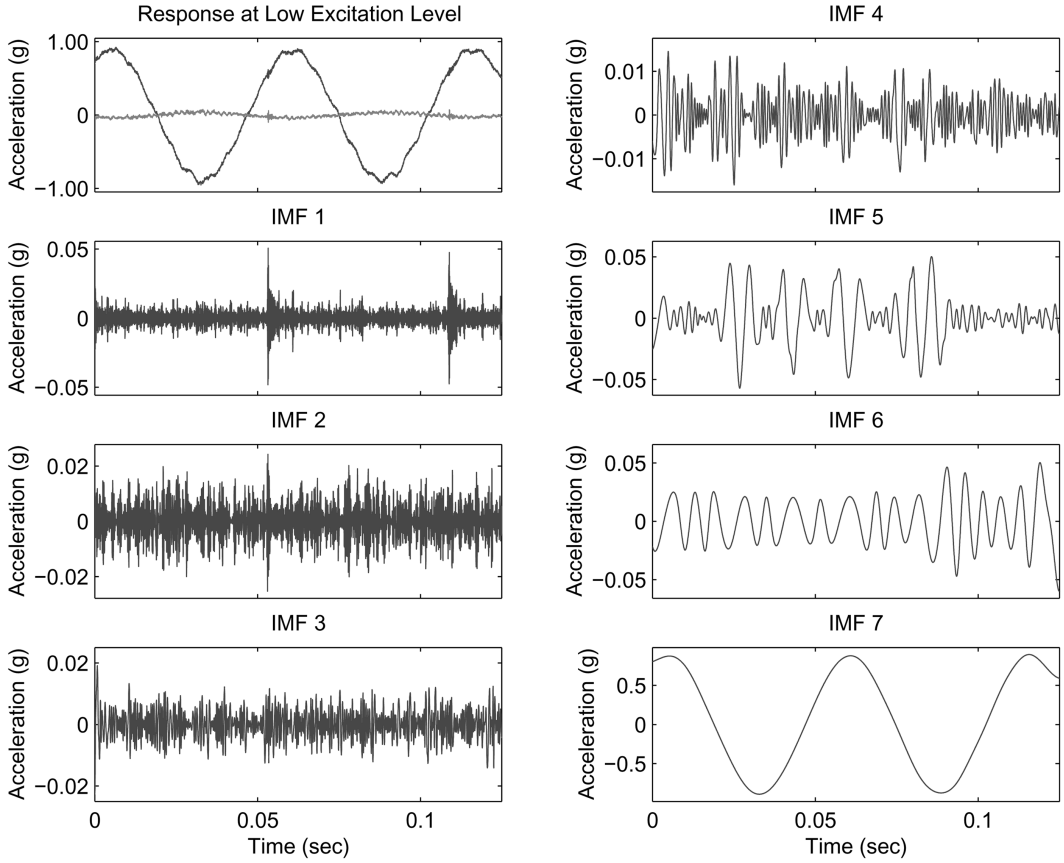

Fig. 5 The acceleration response at the lowest excitation level, and the intrinsic mode functions (IMF) of the in-axis response computed by the empirical mode decomposition

from different IMFs are always mutually exclusive at any given time points. Therefore, the EMD decouples a signal into several basis functions that have mutually exclusive frequency contents. More details on the EMD can be found in Huang *et al*. (1998). This feature of the EMD clearly separates the rattle from the low frequency base excitation. In Fig. 5, the in-axis acceleration response at the lowest excitation level is decomposed into 7 IMFs. The spikes in the first IMF clearly indicate the locations of the rattle. In fact, the first IMF is the time response associated with the rattle. Although it is not presented here, it is a trivial matter to establish an automated rattle identification procedure from the first IMF. For instance, a simple process control chart (Sohn *et al*. 2000) can be easily applied to the first IMF. Using a segment of the time series without rattling, the upper and lower control limits of a control chart can be constructed from an assumed or empirical distribution of the time series segment. Then, the time response of the first IMF at the rattle time points will obviously exceed the control limits automatically identifying the rattle. Another interesting observation is that the last IMF (IMF 7 in Fig. 5) is almost identical to the base excitation at 18 Hz. It should be noted that the maximum amplitude of the rattle shown in the first IMF of Fig. 5 is about 0.05 g, and this amplitude is less than 6% of the harmonic amplitude (about 0.9 g) of the base excitation shown in the last IMF of Fig. 5. Despite the very small amplitude of the rattle, the separation of the rattle and the base excitation was possible because their frequency contents were so distinctive. Although it is not reported here, similar results are found from the in-axis responses of the intermediate and highest excitation levels. In both cases, the first IMF clearly indicated the rattle and the final IMF reconstructed the base excitation function. In this example, both the Holder exponent and EMD were successful in identifying the rattle caused by the moving internal component with unsymmetrical bumpers.

3.2 Acceleration time signals from a loosened bolted connection

The next structure tested is a three-story frame structure model shown in Fig. 6. The structure is constructed of Unistrut columns and aluminum floor plates. The floors are 1.3-cm-thick (0.5 in) aluminum plates with two-bolt connections to brackets on the Unistrut. The base is a 3.8-cm-thick (1.5 in) aluminum plate. Support brackets for the columns are bolted to this plate and hold the Unistrut columns. Dimensions of the test structure are displayed in Fig. 6. All bolted connections are tightened to a torque of 0.7 N-m (60 inch-pounds) in the undamaged state. Four Firestone air mount isolators, which allow the structure to move freely in horizontal directions, are bolted to the bottom of the base plate. The isolators are inflated to 140-kPa gauge (20 psig) and then adjusted to allow the structure to sit level with the shaker. The shaker is coupled to the structure by a 15-cm-long (6 in), 9.5-mm-diameter (0.375-in) stinger connected to a tapped hole at the mid-height of the base plate. The shaker is attached off-center, so that both translational and torsional motions can be excited.

The structure is instrumented with 12 piezoelectric single-axis accelerometers, one per joint as shown in Fig. 6. The accelerometers are oriented to measure vertical accelerations and mounted on the aluminum blocks that are attached by hot glue to the plate. The accelerometers are numbered from the top floor to the first floor and from the right side of the structure to left. Furthermore, the accelerometers at the front of the structure have even channel numbers, while the accelerometers on the back have odd numbers. The nominal sensitivity of each accelerometer is 1 V/g. A 10-mV/lb force transducer is mounted between the stinger and the base plate. This force transducer is used to measure the input to the base of the structure.

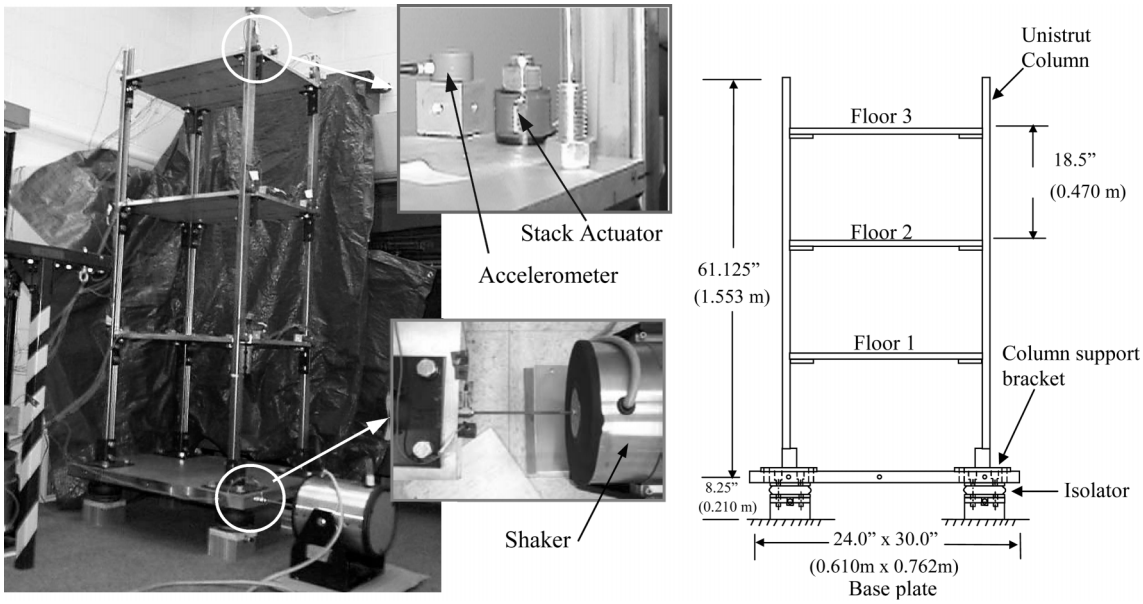

Fig. 6 A three-story frame structure instrumented with accelerometers and a piezoelectric stack actuator

A piezoelectric stack actuator was inserted in the bolt near channel 2 as displayed in Fig. 6. The preload of the bolt was changed by varying the voltage applied to the stack actuator. The expansion of the stack actuator was proportional to the voltage applied. The stack was initially activated by applying approximately 800 V to the stack. Then, the bolt was tightened to a torque value of 16.9 N-m as were all other bolts on the structure. While the structure was excited at the base level by a broadband random excitation generated by the shaker, the stack was deactivated by decreasing the applied voltage to near 0 V, causing the stack to contract and relieve a fraction of the preload in the bolt. That is, the actuator is employed in this example to simulate the loosening of a bolt. Square wave voltage signals generated by a commercial pulse generator caused the stack to expand and contract at specified intervals. Then, a commercial data acquisition system controlled from a laptop PC was used to digitize the accelerometer and force transducer analogue signals. The 32 second acceleration time signals analyzed in this example consisted of 8192 time points yielding a Nyquist frequency of 128 Hz.

The success of the Holder exponent in this example mainly depended on the type of the base excitation. When the structure was driven by a sinusoidal input, the Holder exponent successfully detected the loss of preload in the bolt. The next type of excitation into the three-story structure was a broadband random input that varied from 0 to 1000 Hz. In this environment, any changes in the Holder exponent related to a damage event were not significant compared to other extraneous changes in the Holder exponent. It should be noted that the Holder exponent was originally designed to detect a broadening of the frequency domain response in higher frequency content caused by a discontinuity. However, when a broadband input signal is already applied to the system like this example, the subtle broadening of the frequency content caused by the discontinuity is often masked.

Armed with the insight about the inability of the Holder exponent to detect discontinuities in the

presence of a broadband excitation, the three-story structure was revisited. By limiting the bandwidth of the random input from 0 to 100 Hz, it was hypothesized that the Holder exponent would more easily accentuate the high frequency content resulting from a discontinuity. First a baseline response is obtained from the channel 2 accelerometers when a normal voltage of 800 V is applied to the stack actuator. Then, the square wave voltage signal is alternated between 0 and 800 V as shown in Fig. 7(a), and the corresponding test acceleration response at channel 2 is recorded. Any drop in the voltage applied to the piezoelectric stack corresponds to a loss of bolt preload.

The Holder exponent is applied to the test acceleration signal to examine whether the Holder exponent can locate time points associated with the sudden voltage drops and/or jump shown in Fig. 7(a). A complex-valued Morlet wavelet with length 32 and 64 scales between 0 Hz and the Nyquist frequency (128 Hz) are used for the computation of the scalogram. Again, the mirrored continuous wavelet transform and averaging of the Holder exponent with a moving window size of 8 were applied to minimize the end effect of the wavelet transform and to obtain a smoother Holder exponent plot, respectively. The result of the Holder exponent analysis is reported in Fig. 7(b). The sudden voltage drops near 9.21 and 28.37 seconds are clearly identified by the downward spikes in the Holder exponent plot shown in Fig. 7(b). Next, the automated discontinuity detection algorithm

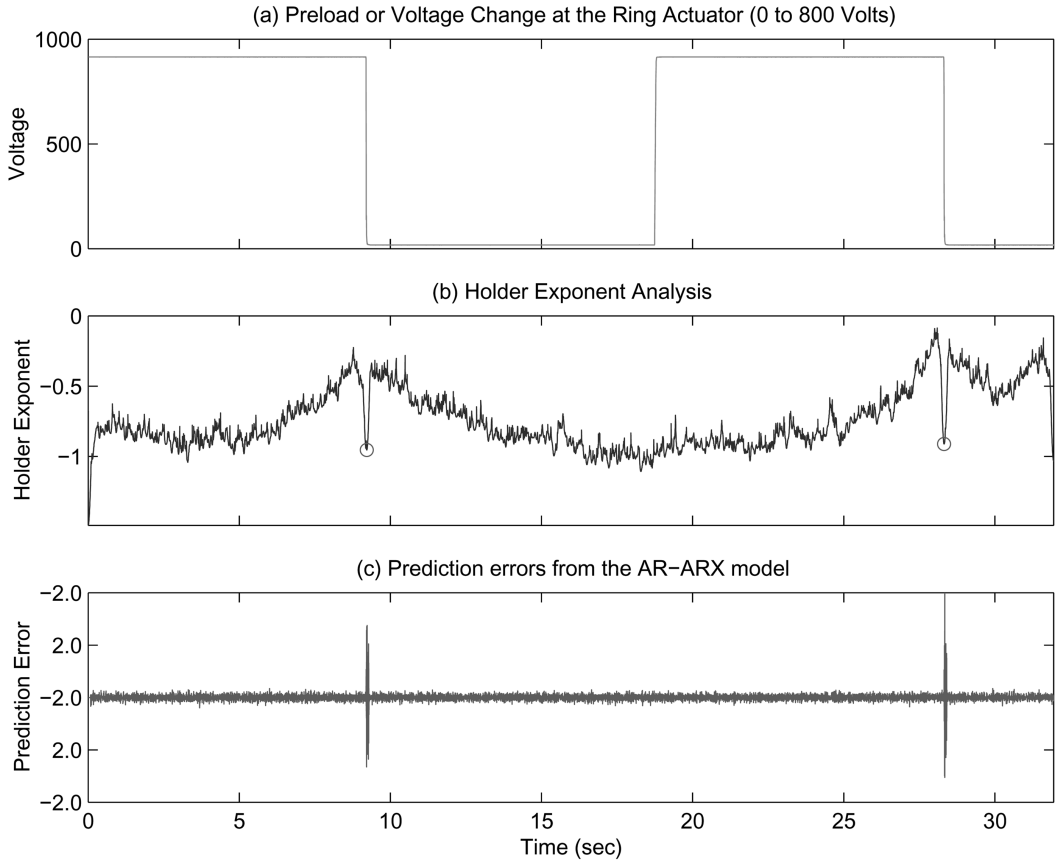

Fig. 7 Detection of preload changes using the Holder exponent and AR-ARX model

is applied to the Holder exponent plot in Fig. 7(b). The baseline signal is used to establish the threshold value for the discontinuity classifier, and the discontinuity points identified by the discontinuity classifier are marked by the circles, which well coincided with these two spike points. However, the Holder exponent completely missed the voltage jump from near 0 to 800 V occurring around 18.78 second. It is speculated that, while the contraction of the actuator caused by an abrupt drop in the applied voltage produced a sudden preload decrease, the expansion of the actuator back to the normal preload state took a much longer time causing a gradually change in the preload. That is, the compression force applied to the actuator by the tightened bolt prevented the instantaneous expansion of the stack actuator resulting in a gradual preload change.

Next, an Auto-Regression and Auto-Regression time series analysis with exogenous inputs (AR-ARX) is employed to substantiate the result of the Holder exponent analysis (Sohn and Farrar 2001). The AR-ARX model is a linear, time predictive model from which residual errors are calculated. These residual errors are used as the features that are monitored. The AR-ARX model is first fit to the baseline signal. The fitted AR-ARX model was then used to compute a sequence of prediction errors from the testing signal. The underlying assumption is that the errors on the abnormal sequence will be significantly higher than those on the baseline sequence because the AR-ARX model is developed from fits to the baseline data. That is, when a time prediction model is constructed from the baseline signal, this prediction model should be able to properly predict the new signal if the new signal is close to the baseline signal. On the other hand, if the new signal were recorded under an abnormal condition different from the condition where the baseline signal was obtained, the corresponding prediction errors would significantly increase.

In this example, p, a, and b values of the AR-ARX model are set to 25, 20, and 5, respectively. Here, p is the order of the auto-regressive model fit in the first step, and a and b are the orders of the auto-regressive and moving average terms of the auto-regressive model with exogenous inputs fit in the second step. For the detailed definition of these parameters, the readers are referred to Sohn and Farrar (2001). The transient nature of the AR-ARX time prediction model at a few initial time points engenders anomalously high initial residual errors, which are duly truncated. First, the AR-ARX model is constructed by fitting it to the baseline signal. Then, the prediction errors on the testing signal are computed and reported in Fig. 7(c). The findings of the AR-ARX time series analysis agree with the results of the Holder exponent again missing the abrupt voltage jump near 18.78 second. Therefore, it is concluded that the expansion of the stack actuator does not produce an instant change in the measured response signal. Finally, it should be straightforward to develop any automated detection procedure based on the prediction errors obtained from the AR-ARX model because the changes are substantial.

3.3 Strain signals during construction of the Singapore-Malaysia Second Link Bridge

Finally, the Holder exponent analysis is used to assess the impacts of several events identified during construction of the Singapore-Malaysia Second Link Bridge (see Fig. 8). This bridge is known as the “Second Link” as it is the second land crossing built between the two countries after the Johor Causeway, which was constructed in the 1920s. This bridge is a post-tensioned box girder bridge carrying a dual carriageway with three lanes on each carriage. The bridge was completed in 1997 and opened to traffic in the same year. A structural health monitoring system was installed during construction of the bridge to monitor the bridge’s short-term and long-term behavior and performance under construction loads, environmental loads, and vehicular loads. The sensing system

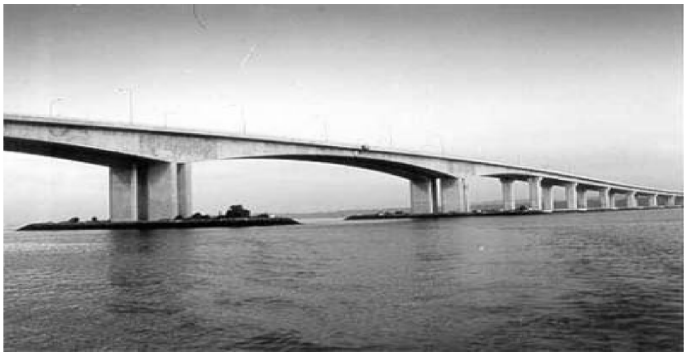

Fig. 8 Singapore-Malaysia Second Link Bridge (Courtesy of Moyo and Brownjohn 2002)

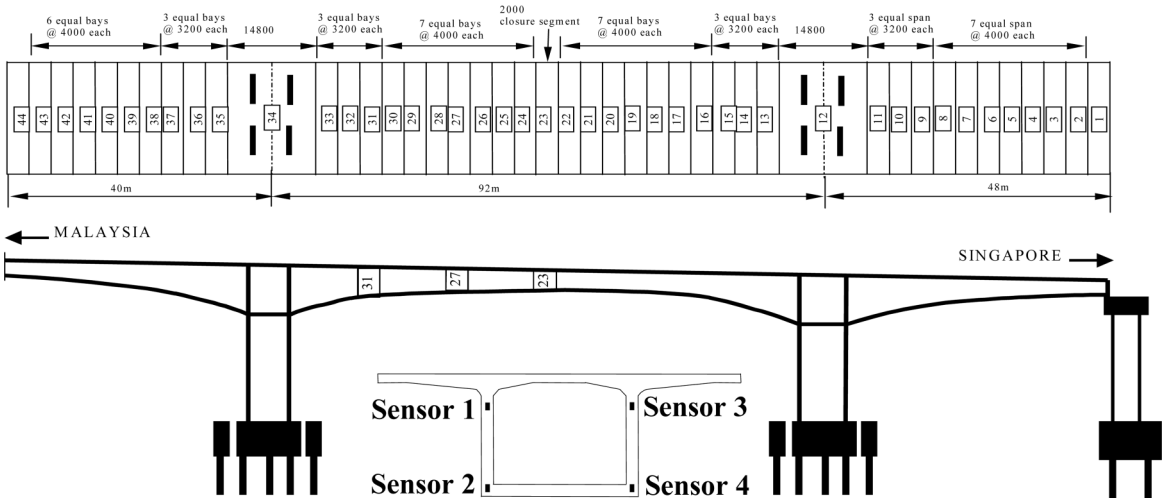

Fig. 9 Layout of the Singapore-Malaysia Second Link Bridge (Courtesy of Moyo and Brownjohn 2002)

installed includes a set of temperature sensors, load cells, strain gauges and accelerometers distributed in three segments of the bridge's main span on Singapore side. Details of the Second Link Bridge monitoring system can be found in Brownjohn and Moyo (2000).

In this example, strain data recorded from strain gauges embedded into one of the concrete segments are used to identify several events during the construction phase of the bridge. These events include post-tensioning, concreting of segments, and shifting of form traveler. (The form traveller moves out from the tower one segment at a time. The primary purpose of the form traveller is to hold the wet concrete in place until it hardens into the proper shape. The form must then be stripped from the hardened concrete. To achieve this, all surfaces of the form are able to move.) The strain data hourly measured from April 29th, 1997 to June 1st, 1997 (800 time points) are used in this study. Specifically, the strains were recorded from four sensor locations within segment 31. The location of segment 31 and sensor positions are displayed in Fig. 9. The time of the construction events of interest are listed in Table 1. The strain signals from the four sensors of bridge segment 31 are shown in Fig. 10. The observation of Fig. 10 reveals that the concrete casting yields a sudden

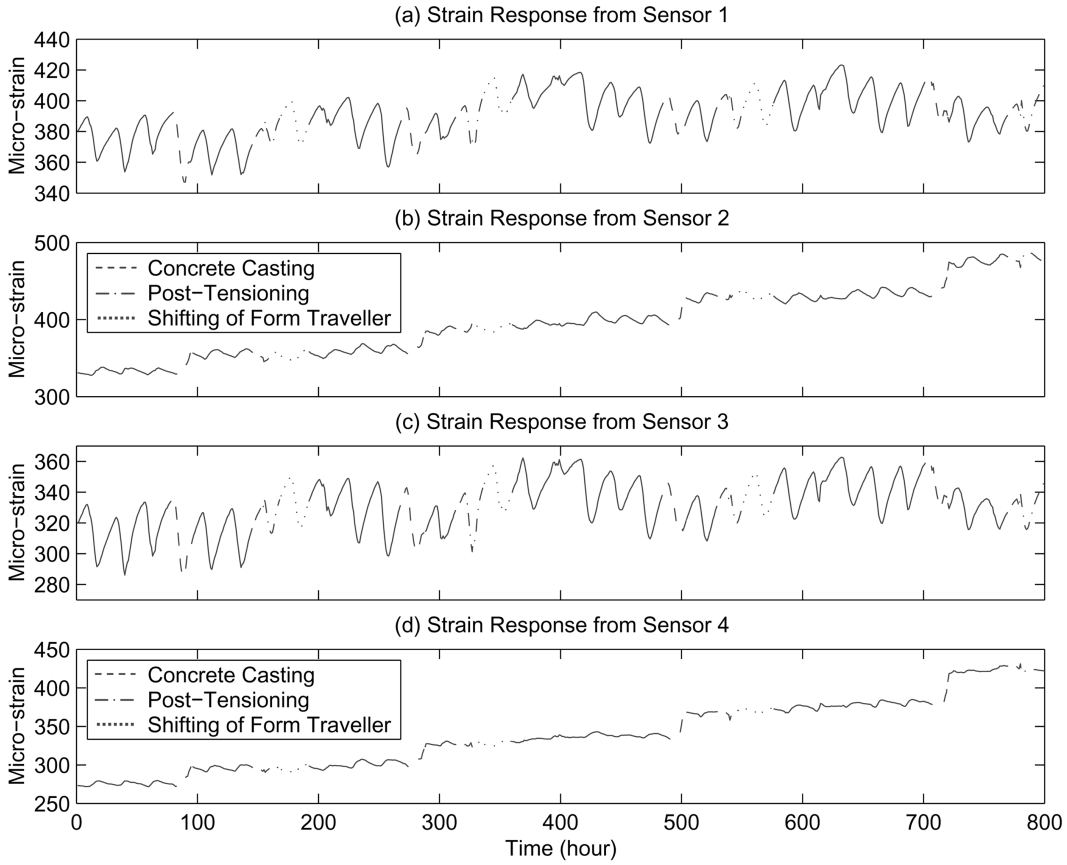

Fig. 10 Strain gauge readings from the four sensors within the bridge segment 31

Table 1 Concreting, post-tensioning, and shifting of form traveller during construction

Activity	Activity time (hours from 12:00AM, April 29th, 1997)			
	Segment 27	Segment 26	Segment 25	Segment 24
Concreting	91-95	280-288	496-500	700-710
Post-tensioning	155-156	328-329	538-540	778-779
Shifting of form traveller	180-182	352-355	553-558	950-954

jump in strain for the strain signals from sensor locations 2 and 4. However, this abrupt strain increase is not obvious from the strain signals from sensor locations 1 and 3. In addition, the event of post-tensioning and shifting of form traveler are hard to visually identify.

The Holder exponent is applied to all four signals and the results are reported in Fig. 11. Again, the discontinuities identified by the automated classifier are marked by the circles. A complex-valued Morlet wavelet with length 4 is used for the scalogram, and 64 scales are used. Other parameters for the Holder exponent are kept same as the previous examples. Several findings are made from Fig. 11. First, the event of concreting and post-tensioning of segments are successfully

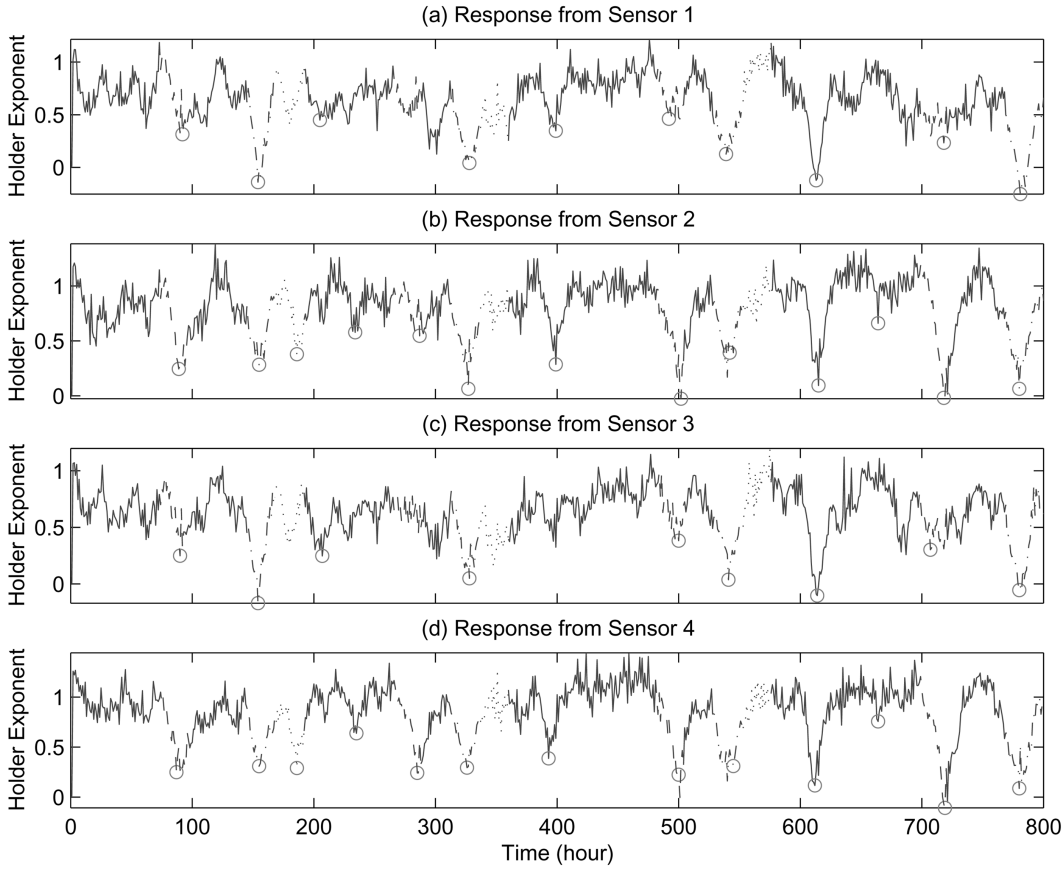

Fig. 11 Holder exponent analysis of the bridge strain gauge data (-------: concrete casting events; - - - - - - -: post-tensioning events; ·····: shifting of form traveler)

identified from all four-sensor readings. However, the shifting of the form traveller does not seem to be related to the discontinuities in the measured signals. The authors believe that the form traveller shifting does not necessary cause significant abrupt changes in the measured strain data. Second, the post-tensioning event is the most noticeable event from all four sensors. The concreting of segments is more discernable from sensors 2 and 4 rather than sensors 1 and 3. This result agrees well with the visual inspection of the raw strain data shown in Fig. 10. In addition, it is believed that there were other unknown sharp changes in the signals near 390 and 720 hours. This observation coincides with the findings reported in Moyo and Brownjohn (2000). It should be interesting to go back to the construction log book and to see if there were any particular events near these two time points.

4. Conculsions

In this study, a Holder exponent analysis is successfully applied to various experimental signals to detect discontinuities in the measured response data that can potentially be introduced by certain

types of damage. Examples of signals being analyzed include the acceleration response of a mechanical system subjected to a harmonic excitation with a rattling internal part, the acceleration signals of a three-story building model with the preload of a bolt being controlled by a piezoelectric actuator, and the strain records of the Singapore-Malaysia Second Link Bridge exposed to concreting and post-tensioning of segments and shifting of form traveller during construction. Furthermore, a discontinuity classifier is developed to automate the identification procedure of discontinuities. The results of the Holder exponent analysis are also confirmed by other signal processing techniques including the empirical mode decomposition and auto-regressive time series analysis. The simplicity and data driven nature of the proposed approach makes it very attractive for embedding the discontinuity algorithm into a digital signal processing chip or field programmable gate array, which can be an integrated part of an intelligent sensor unit with micro-electromechanical system (MEMS) sensors, a wireless telemetry, on-board computation power and a battery.

However, further research regarding the use of the Holder exponent for damage detection needs to be explored. For instance, the establishment of the threshold value of the discontinuity detection algorithm is currently a case-by-case basis taking into account the specific properties of the signals being monitored. In addition, there is no principled guideline for the selection of the mother wavelet, the width of the wavelet, and the number of scales being used for the wavelet transform. The automation of the parameter selection would be an area of future study. This automation step could not be fully tackled in this study because of the limited amount of normal condition data available for training the discontinuity detection algorithm.

Acknowledgements

The authors would like to thank Nguyen B. Do, Scott R. Green, and Timothy A. Schwartz for conducting the experimental tests of the three-story building model presented in this paper as part of their Los Alamos Dynamics Summer School Project. The authors also thank Pilate Moyo and James M.W. Brownjohn for providing the strain measurement data of the Second Link Bridge and offering their valuable comments. This work is supported by Los Alamos Laboratory Directed Research and Development (LDRD) funds.

References

Brownjohn, J.M.W. and Moyo, P. (2000), "Monitoring of Singapore-Malaysia Second Link during construction", *Proc. of the 2nd Int. Conf. on Experimental Mechanics*, Singapore, Nov. 29-Dec. 1, 528-533.

Hambaba, A. and Huff, A.E. (2000), "Multiresolution error detection on early fatigue cracks in gears", *IEEE Aerospace Conference Proceedings*, **6**, 367-372.

Huang, N.E., Shen, Z., Long, S.R., Wu, M.C., Shih, H.H., Zheng, Q., Yen, N.C., Tung, C.C. and Liu, H. (1998), "The empirical mode decomposition and the Hilbert spectrum for nonlinear and non-stationary time series analysis", *Proc. R. Soc. Lond. A*, **454**, 903-995.

Mallat, S. and Hwang, W.L. (1992), "Singularity detection and processing with wavelets", *IEEE Transactions on Information Theory*, **38**, 617-643.

Peng, Z., He, Y., Chen, Z. and Chu, F. (2002), "Identification of the shaft orbit for rotating machines using wavelet modulus maxima", *Mechanical Systems and Signal Processing*, **16**(4), 623-635.

Robertson, A.H., Farrar, C.R. and Sohn, H. (2003a), "Singularity detection for structural health monitoring using holder exponents", *Mechanical Systems and Signal Processing*, **17**(6), 1163-1184.

Robertson, A.N., Sohn, H. and Farrar, C.R. (2003b), "An improved statistical classifier for identifying signal discontinuities using holder exponents", *The 4th International Workshop on Structural Health Monitoring*, September 13-17, Stanford, CA.

Shekarforoush, H., Zerubia, J. and Berthod, M. (1998), "Denoising by extracting fraction order singularities", *IEEE International Conference on Acoustics, Speech and Signal Processing*, **5**, 2889-2892.

Sohn, H., Czarnecki, J.J. and Farrar, C.R. (2000), "Structural health monitoring using statistical process control", *J. Struct. Eng.*, ASCE, **126**(11), 1356-1363.

Sohn, H. and Farrar, C.R. (2001), "Damage diagnosis using time series analysis of vibration signals", *Smart Materials and Structures*, **10**, 446-451.

Sohn, H., Farrar, C.R., Hemez, F.M., Czarnecki, J.J., Shunk, D.D., Stinemates, D.W. and Nadler B.R. (2003), "A review of structural health monitoring literature: 1996-2001", Los Alamos National Laboratory Report, LA-13976-MS, 2003.

Struzik, A. (2001), "Wavelet methods in (financial) time-series processing", *Physica A*, **296**, 307-319.

Wong, K.Y., Chan, W.Y., Man, K.L., Mak, W.L.N. and Lau, C.K. (2000), "Structural health monitoring results on Tsing Ma, Kap Shui Mun, and Ting Kau Bridges", *Proceedings of SPIE*: Nondestructive Evaluation of Highways, Utilities, and Pipelines (Vol. 3995), Newport, CA.